JACS
JOURNAL OF THE AMERICAN CHEMICAL SOCIETY

ARTICLE

pubs.acs.org/JACS

Influence of Binding Groups on Molecular Junction Formation

Carlos R. Arroyo,[†,§] Edmund Leary,[‡,∥] Andrés Castellanos-Gómez,[†] Gabino Rubio-Bollinger,[†] M. Teresa González,[*,‡] and Nicolás Agraït[†,‡,¶]

[†]Departamento de Física de la Materia Condensada and [¶]Instituto "Nicolás Cabrera", Universidad Autónoma de Madrid, E-28049 Madrid, Spain

[‡]Instituto Madrileño de Estudios Advanzados en Nanociencia (IMDEA-Nanociencia), Ciudad Universitaria de Cantoblanco, E-28049 Madrid, Spain

Supporting Information

ABSTRACT: We study the formation mechanism of molecular junctions using break-junction experiments. We explore the contribution of gold-atom rearrangements in the electrodes by analyzing the junction stretching length, the length of individual plateaus, and the length of the gold one-atom contacts. Comparing the results for alkane dithiols and diamines, we conclude that thiols affect gold electrode dynamics significantly more than amines. This is a vital factor to be considered when comparing different binding groups.

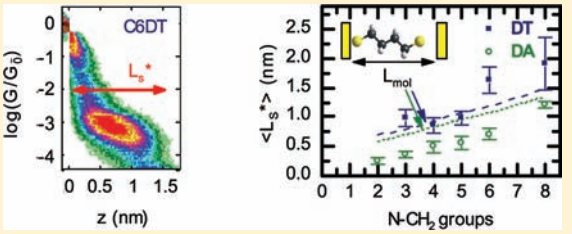

INTRODUCTION

Great efforts have been made in molecular electronics toward understanding electron transport through an isolated molecule attached between two metal electrodes. Conventional methods to wire molecules rely on their self-assembly on an electrode surface. Whenever two electrode tips are closer than the total length of the molecule, one, or more, of these molecules can self-assemble bridging the gap, and forming a molecular junction. The most widely used techniques to achieve this are based on the break-junction (BJ) technique.[1] Using mechanically controlled BJ[2] or scanning tunneling microscope (STM) BJ,[3] the distance between two atomically sharp gold electrodes can be controlled with picometer resolution. In these devices, the geometry of the electrode tips, the binding configuration, and the number of assembled molecules are uncontrolled variables, and consequently depend on the circumstances of each molecular junction realization. Therefore, single-molecule conductance experiments rely on statistical analyses of a large number of equivalent molecular junctions.[3−6]

In the case of simple alkane molecules, the resulting conductance, G, distribution spreads over approximately 1 order of magnitude. The origin of this broad distribution is still under debate, but factors which have been considered are possible differences in binding between the molecule and the metal electrode, conformational changes of the alkane, or a large dispersion on the total number of attached molecules.[7−13] The chemical group used as anchor for the self-assembly can be crucial in obtaining reproducible molecular junctions. It has been shown, for example, that amines produce narrower G distributions than thiols.[14,15]

On the other hand, the formation process of molecular junctions has been little explored, and the key parameters controlling the process have not yet been entirely identified. Studying the stretching distance over which G is observed to be constant, it is possible to compare the stability of different binding groups,[15,16] or identify different junction breaking mechanisms.[17−19] Also, to include an additional modulation in the electrode movement allows exploring the stability of different binding geometries.[20−22]

A molecular junction is formed by two parts: namely, the molecules and the metallic electrodes. In a break-junction experiment, the electrodes are reformed and reorganized in each experiment, and the contribution of this on the mechanical properties of the junctions has mainly been neglected. To characterize the system properly, especially when comparing junctions based on different compounds, we need to identify the contribution of the molecules and electrodes separately, as well as how they interact with each other. In this paper, we aim to understand the contribution of electrode deformations on the junction formation process, by analyzing the profile of the G variation with the stretching distance z on STM-BJ experiments. On the basis of results for a family of alkane dithiols, CnDT, and diamines, CnDA (with n = 2, ..., 6, 8 for each family), we perform a statistical analysis of the maximum stretching distances that the molecular junctions can withstand, the maximum length of individual plateaus, and the stretching length of the gold one-atom contact. Our analysis allows us to identify the important role of gold atom rearrangements, and how these are modified by the presence of different molecules on the electrode surfaces.

EXPERIMENTAL SECTION

Our experimental setup consists of a home-built STM operated at room temperature. We use commercial gold substrates on quartz (Arrandee). For cleaning the surface of gold, the substrate is immersed

Received: March 1, 2011
Published: August 01, 2011

for 2 min in a freshly prepared piranha solution (1:3 H_2O_2 (33%) in H_2SO_4 (98%)). After the piranha treatment, the substrate was rinsed several times with Milli-Q water and dried in a stream of nitrogen gas. Then, the gold surface was flame annealed with a butane burner for 1−2 min. The tip consists of a freshly cut gold wire (99.99% purity) of 1−1.5 mm in length and 0.250 mm in diameter. Gold nanocontacts are formed and broken repeatedly by moving the STM-tip toward and away from the substrate at 16 nm/s. The evolution of contacts is monitored by means of the conductance, $G = I/V$, when a bias voltage of 25 mV (80 mV for C8DA) is applied between the tip and the substrate. The molecules were deposited on a clean gold substrate by adding a droplet of 2 μL of 1 mM solution freshly prepared in 1,3,5-trichlorobenzene (TCB). The low volatility of this organic solvent at room temperature allows us to perform measurements for a long time using a small volume of liquid. For continuously measuring more than 5 orders of magnitude in conductance, we have built a linear current-to-voltage converter with two amplification stages.

RESULTS AND DISCUSSION

For each molecule, we have performed several thousand individual breaking cycles, obtaining typical G versus z traces, as shown in Figure 1. In the traces, a plateau at $G_0 = 2e^2/h$ provides the evidence for the formation of a one-atom contact, during the last stage of the gold-nanocontact breaking, which leaves two atomically sharp electrodes. A series of plateaus at lower G values are the signature that one or more molecules have self-assembled between the electrodes, forming a molecular junction.[3] Figure 2 summarizes the 2D histograms[16,23] performed with a group of 5000 G versus z traces for each molecule. To compute these histograms, the traces have been shifted along the z-axis to fix $G(z=0) = 0.5\ G_0$, and constant bin widths of $\Delta\log(G/G_0) = 0.06$ and $\Delta z = 0.013$ nm were used. In the plot, the color scale indicates the number of counts in each $\Delta\log(G/G_0) - \Delta z$ interval, normalized to the number of curves used to build the histograms. The color scale has been chosen to highlight events with low probability, which frequently correspond to the signature of molecular junction formation. The same color scale has been used in all the histograms presented in this paper. The exponential G decay due to tunneling between the electrodes shows in the histograms as a straight color band. On the other hand, a definite prominence in all the histograms, except C2DT, identifies the region where plateaus develop in the majority of traces.

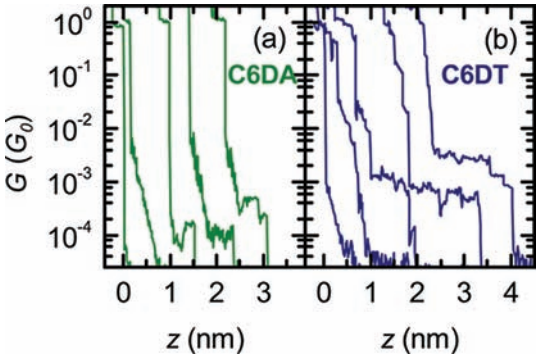

Figure 1. Individual G vs z traces for hexane with two anchoring groups, amines (a) and thiols (b). Plateaus for the dithiol are longer and at higher conductance. After the gold plateau at 1 G_0, the gold atoms are fast relaxed in the presence of the diamine (abrupt conductance decay). The relaxation occurs in several steps in the presence of the dithiol.

From an inspection of Figure 2 we see that, inside an anchor-group family, the molecular plateaus are centered at a lower conductance value and spread to longer stretching distances as n increases (the variation of G with n is shown in detail in the Supporting Information). We also see that, for a given n, mean G values and stretching distances are lower for diamines than for dithiols. We find several reports in the literature discussing the G-distribution for both alkane-dithiols and diamines.[7−12,24] In this paper, we focus on the stretching length analysis.

Apparent Stretching Length. Binding configurations in a molecular junction can be very different, resulting in a variety of final electrode−electrode distances. At the time a molecular junction breaks, the maximum for this distance will correspond to the case of an extended molecule placed between the apexes of the electrodes, L_{mol}.[25] Therefore, for completely rigid electrodes (no deformations), we expect the total stretching length of the junctions (measured from the position at which a gap between the electrodes starts to open, until the last molecular plateau breaks) to be lower than or equal to L_{mol}.

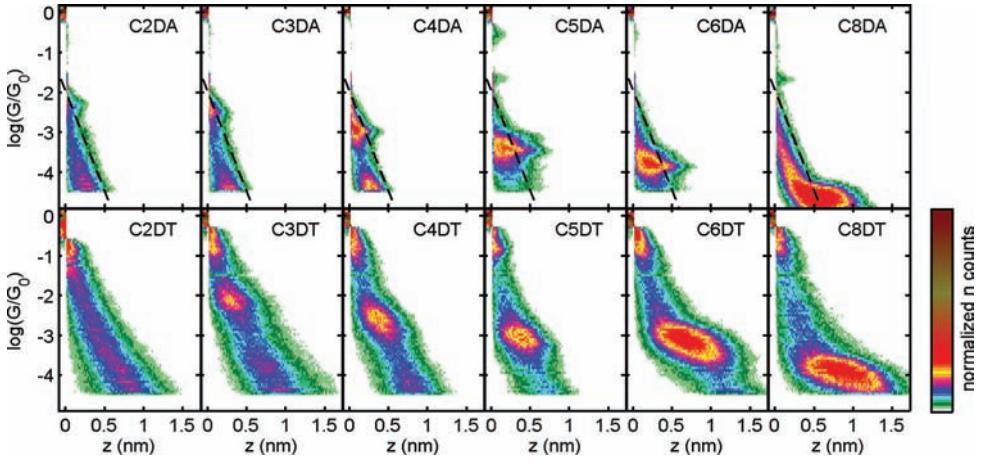

Figure 2. 2D histograms of alkane diamines (CnDA) and alkane dithiols (CnDT). For all the molecules, except C2DT, a prominence in the histogram indicates the G values and stretching distances at which most of the plateaus develop in the individual G vs z traces. The dashed lines in the diamine histograms correspond to the expected tunneling curve passing through 1 G_0 at $z = -0.4$ nm, for a tunneling barrier of 1.3 eV. The color scale shows the number of counts normalized to the number of traces included in the histograms.

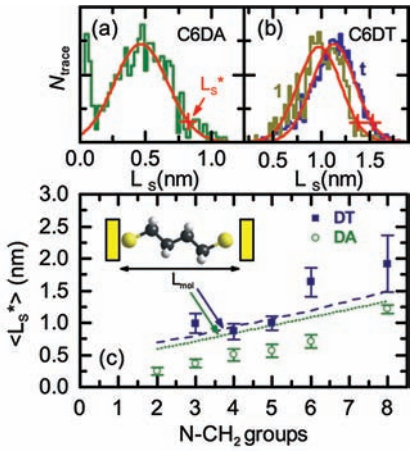

Figure 3. Apparent stretching length L_S distribution of a measurement of C6DA (a) and C6DT (b) (t, total set of traces; 1, only traces with sharp G decay after 1 G_0). The red lines correspond to Gaussian fits to the data. L_S* is the distance at which the distribution decays to 20% of its maximum (red crosses). (c) Variation of $\langle L_S^* \rangle$ with the number of carbons in the alkane. $\langle L_S^* \rangle$ is the averaged L_S* over several measurements. The lines are the calculated molecular lengths[25] L_{mol} for DT (dashed) and DA (dotted).

For our analysis, we define the total apparent stretching length for each trace, L_S, as the length interval going from just after the gold-contact breakage (G_1 = 0.5 G_0) to a G_2 below the region where the molecular plateaus end. This G_2 is chosen to be, for each molecule, below the molecular peak on the conductance histograms, as shown in the Supporting Information. Note that this magnitude is not the plateau length used in other studies.[15−17,24] We choose this magnitude to perform a direct comparison with the molecular length L_{mol}. Figure 3a,b shows the distribution of L_S values for two groups of consecutive traces. We are interested in those molecular junctions with a molecule fully stretched between the electrodes. As these will contribute to the far right of the distribution, we characterize the measurement by an L_S*, defined as the L_S at which the distribution has decayed to 20% of its maximum (red crosses in the figure). This value is well above the final tail of the Gaussian, where the probability decays slowly. Figure 3c shows the variation of this magnitude with n for both dithiols and diamines. To explore measurement-to-measurement variations, we have calculated the value of L_S* from measurements at different locations on the substrate and on different experimental runs. In Figure 3c, $\langle L_S^* \rangle$ was calculated for each molecule as the average of these. The error bars indicate the standard deviation from the mean value. In addition, we have plotted the calculated molecular length[25] L_{mol} as dashed (thiols) and dotted (amines) lines.

Figure 3c shows that, for diamines, $\langle L_S^* \rangle$ varies with n with same slope as L_{mol}, but located ∼4 Å below. The standard deviation for all the family stays below 1 Å. On the hand, for dithiols, the increasing trend of $\langle L_S^* \rangle$ with n is faster and fluctuates significantly. We find large measurement-to-measurement variations, which translates into standard deviations of up to 4 Å. However, what is especially striking is that for the longest dithiols, C6DT and C8DT, $\langle L_S^* \rangle$ is significantly longer than L_{mol}.

So far we have not considered any deformation at the gold electrodes. However, from experiments on gold nanocontacts,[26−28] we know that gold suffers deformations under a pulling stress. Just after the breakage of the gold contact, which is our zero in z, the electrodes are not relaxed, but still accumulate the stress of the last elastic stretching of the Au−Au bonds.[27,28] For a gold nanocontact in vacuum, this stress is relaxed by a sudden retraction of the electrodes of approximately 4 Å (using the values of ref 29 corrected as indicated in ref 30). This includes pure elastic relaxation of the stretched Au−Au bonds,[31] and also rearrangements of Au atoms at the apexes. We denote by d the whole gold atom relaxation distance after the gold nanocontact breaks.

As the electrodes move apart, the molecules attached to both electrodes will be extended and stretched. If the anchoring group binds the molecules to gold strongly enough, at the last stage of the junction stretching, the Au−Au bonds at the electrodes can be elastically elongated again, or some atoms may be displaced, resulting in an extra stretching distance d'. Taking these gold-deformation contributions into account, the *true* maximum stretching length of a molecular junction would be $L_{mol} + (d' - d)$.

Note that in principle the alkane chain could also be elastically stretched during the pulling. However, the spring constant of an alkane chain is considerably large (520 N/m for a C−C bond, 249 N/m for a C−S bond, and 120 for an S−Au bond).[32] A gold contact breaks under a force of 1.5 nN.[28] Before reaching this force, even for a chain of 8 carbon atoms, the maximum stretching would be below 1 Å. Thus, we can neglect any elastic stretching of the molecules in our measurements.

In Figure 2, we see that for amines there is an abrupt conductance decay just after the gold contact breakage, which is also clear in the individual traces of Figure 1a. This indicates that the gold electrodes have indeed retracted by some distance d. The dashed black lines in Figure 2 correspond to the tunneling decay expected for a retraction of 4 Å, using a typical tunneling barrier for TCB of 1.3 eV (obtained from 1D conductance histograms as shown in the Supporting Information). The tunneling contribution for diamines falls with the same slope just to the left of this line, showing that the gold retraction in all the curves is at least (or larger than) that at low temperature without molecules ($d \geq 4$ Å). Interestingly, this is approximately the length difference observed between the $\langle L_S^* \rangle$ and L_{mol} values for diamines in Figure 3. Possible explanations for $\langle L_S^* \rangle$ being too short for diamines are the fact that Au−N bonds are too weak to withstand stretching forces,[15] or that the junctions only form far from the apexes. However, the agreement observed here between $\langle L_S^* \rangle - L_{mol}$ and the expected gold electrode retraction, d, suggests that it is possible that diamines form junctions with the molecule stretched at the apexes of the electrodes. Au−N bonds seem to be too weak to force further significant elongation of the electrodes during the molecular junction stretching ($d' \simeq 0$, also recently suggested[33]), and the L_S values appear to be shorter for diamines only because the electrode retraction has opened a real gap around 4 Å longer than the apparent measured value.

The behavior in the presence of dithiols is significantly different from that of diamines. In many of the individual traces (see Figure 1b), the conductance decays slowly after 1 G_0, with several abrupt conductance drops instead of in a single step as in the presence of diamines. This suggests that the presence of thiols over the gold surface hinders the gold retraction, which occurs in several steps and to a lesser extent. To check this model, we have separated the dithiol traces showing an abrupt decay at z = 0 (those which go from 0.5 to 10^{-2} G_0 in less than 1 Å), which are approximately 20% of the total. We expect that, for these junctions, a similar relaxation as in the presence of amines occurred after the gold breakage. Figure 3b compares, for a measurement of C6DT, the L_S distribution for such group of

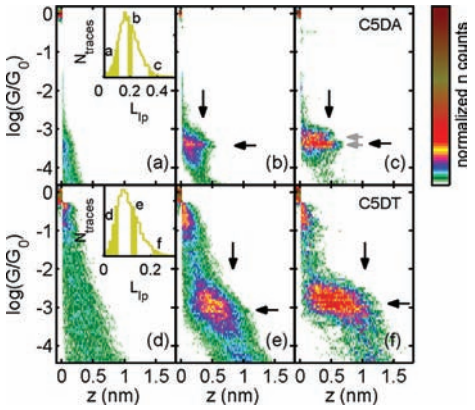

Figure 4. 2D-histograms of groups with different L_{lp} for C5DA (a−c) and C5DT (d−f). The corresponding L_{lp}'s for each 2D-histograms are indicated in the distributions of the insets in panels a and d. The back vertical and horizontal arrows indicate, respectively, the position of $\langle L_S \rangle$ and $\langle \log(G/G_0) \rangle$ for each group of traces. The 2 gray horizontal arrows in panel c indicate the position of two individual peaks for amines, which are frequently distinguished.

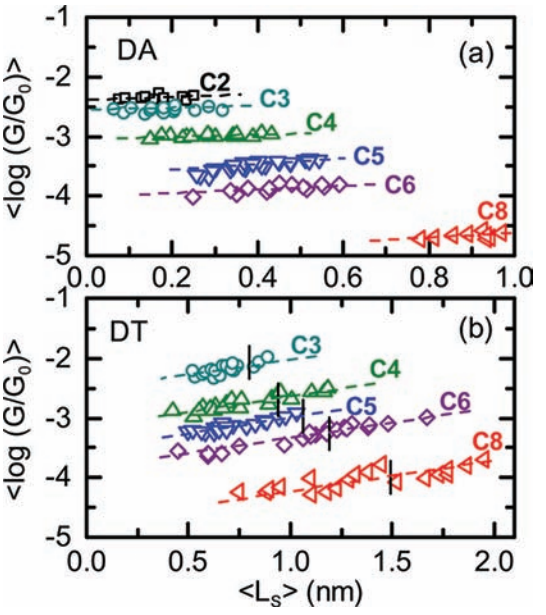

Figure 5. Variation of $\langle \log(G/G_0) \rangle$ with $\langle L_S \rangle$ for different L_{lp} groups, for diamines (a) and dithiols (b). Dashed-lines are guides for the eye. The vertical lines in panel b correspond to the length of the molecules L_{mol}.

traces (labeled with a 1), with the distribution of the total set (labeled with a t). Indeed, the maximum stretching length L_S^* is shorter (by around 2 Å), indicating a larger retraction d for these traces. The same result is consistently observed in all the alkanedithiols.

The fact that, in some cases, $\langle L_S^* \rangle$ values are larger than L_{mol} strongly suggests that, in the presence of the dithiols, not only is the gold retraction compensated, but an extra deformation takes place when stretching the molecular junction, that is, $d' > d$. It has been previously proposed that, when pulling a dithiol molecular junction, a gold atom can be pulled out of the electrode, so that the junction finally breaks at a Au−Au bond.[34] In Figure 3, the stretching lengths for C6DT or C8DT are on average around 5 Å larger than L_{mol}. Moreover, the error bars are large, and for some measurements, L_S^* can be up to 1.5 nm larger than L_{mol}. In such cases, it is unlikely that a single molecule between the electrodes could produce this level of deformation. Even allowing an elastic deformation at the electrodes of several angstroms, a single molecule will have to pull out a gold chain of around 1 nm, which is very unlikely, even at low temperature.[30] This suggests that several molecules in parallel participate in the junctions with the largest L_S. The combined effect of several molecules pulling together from the electrodes is more likely to produce the rearrangement and movement of gold atoms at the electrodes. In the next section, we will show how traces with large L_S display long individual plateaus at high conductance values. This sustains the idea that for those molecular junctions that withstand long stretching lengths there are several molecules in parallel between the electrodes. On the contrary, a single molecule pulling a gold atom out of the surface would be in a 'top' position which is usually associated with the lowest molecular conductance values.[7,12]

Correlation between Junction Conductance and Stretching Length. The individual G versus z traces show a large variety of behaviors, suggesting that different breaking scenarios are possible. To gain insight into the process, we sorted our traces according to their profile. On the basis of the idea that a larger plateau in a trace relates to a more stable molecular junction between the electrodes, we used the length of the longest plateau in each trace L_{lp} as sorting magnitude. In contrast to other studies,[15−17,21,24] we focus only on the longest plateau in each trace and not in each individual plateau (see Supporting Information for a detailed description). Our aim is not to analyze the distributions of individual plateau lengths (with values that depend strongly of the parameters used to define where the plateau starts and ends), but to study separately traces resulting from junctions with different stability.

Groups of traces with different L_{lp} produce distinct 2D histograms as those shown in Figure 4 for C5DA and C5DT (the L_{lp} distributions for the complete set of traces are shown as insets, indicating at which L_{lp} intervals the 2D histograms shown in the figure correspond). Traces with low L_{lp} values show only tunneling contribution, while high L_{lp} means that a stable molecular junction has been formed between the electrodes. We separated all measured traces into groups, dividing the L_{lp} range into intervals 0.025 nm long. For each group, we calculated the mean values of the conductance $\langle \log(G/G_0) \rangle$ and apparent stretching length $\langle L_S \rangle$, from the log$G$-histogram peak, and the L_S distribution (examples are shown in the Supporting Information). As now all curves in the groups have plateaus of similar length, we calculate $\langle L_S \rangle$ for each group, instead of L_S^* as in the previous section (for a summary of the different length parameter definitions, see Supporting Information). In Figure 4, the values of these magnitudes are indicated by black horizontal and vertical arrows respectively. Figure 5 shows the correlation between $\langle \log(G/G_0) \rangle$ and $\langle L_S \rangle$ values.

For diamines, the variation of $\langle \log(G/G_0) \rangle$ with $\langle L_S \rangle$ is small. The slight increasing tendency observed in Figure 5 is due to the development of the second peak at around 1.6 times the conductance of the first, for curves with long L_{lp} (shown for C5DA in Figure 4c). This suggests that diamines form molecular junctions with one or two molecules between the electrodes.

On the other hand, for dithiols, $\langle \log(G/G_0) \rangle$ increases significantly with $\langle L_S \rangle$. For medium L_{lp} (Figure 4e), which

corresponds to low $\langle L_S \rangle$ values in Figure 5b, the prominences spread out in a broader conductance range. There is a decrease of conductance with z, which probably indicates that molecules are detaching rapidly when stretching the junction. The last stages of junction breakage would correspond to a very few, or even one, molecule junction. As L_{lp} increases (Figure 4f), the prominence becomes narrower and more horizontal, being centered at higher conductance values (see Supporting Information for more examples and corresponding 1D histograms). This probably corresponds to stable junctions formed by several molecules strongly attached to the electrodes, which, hence, show a higher conductance. From our results of Figures 4 and 5, we then conclude that the stability of the junctions is due to a large number of molecules bridging the electrodes.

As mentioned above, the histograms for diamines display one or two well-defined peaks. For dithiols, the 1D histograms of curves with a given L_{lp} value frequently have a structure of finer peaks (see Supporting Information). However, this structure was irreproducible in different runs, and fluctuates strongly with small variations of L_{lp}. For a given compound, we have not found any correlation of conductance and stretching length that suggest that molecules bind to gold with different conformations (which would be expected to withstand different stretching). However, if our picture of many molecules participating in the junctions is correct, different molecules can bind to the electrodes in different conformations in a given junction, washing out the signature of each conformation individually.

On the other hand, $\langle L_S \rangle$ values above L_{mol} (L_{mol} is indicated by vertical black lines in Figure 5b) imply that the bridging molecules are working collectively to displace partially some of the gold atoms at the apexes. The fact that $\langle L_S \rangle$ gets especially long for the longest alkane-dithiols implies that they are more prone to displace gold atoms. This is not surprising since longer alkanes can bind between the electrodes more easily, as they can reach points further from the electrode apexes and they are more flexible. Also, larger alkanes have faster assembly kinetics and a larger tendency to pack by van der Waals interactions.[35,36] Their presence can have a mechanical effect even if not all of them are bridging the electrodes. Under a stretching force, the combined effect of these partially packed long molecules will produce rearrangements and movements of gold atoms at the electrodes in an easier way. In Figure 3c, we observed a change of trend in the $\langle L_S^* \rangle$ variation above C5DT. In the formation of self-assembled monolayers, significant changes in the SAM organization are observed when alkanes become longer than 5 carbons.[37] This indicates that there is a threshold for the organization of alkanes on the gold surface at this length, which correlates with our results.

We observed that dithiols tend to form junctions with multiple molecules more frequently than diamines. This phenomenon will also have an effect on the mean values of junction conductance obtained for these compounds. For dithiol, the mean conductance will not correspond to single molecule values, but to the conductance of the most probable number of molecules in the junction.[13] When calculating the simple mean conductance[6,38] for our studied molecules G_{mol}, we find that our decay constant β ($G_{mol} \propto \exp(-\beta n)$) is, for amines, $\beta_{amine} = 0.95\ n^{-1}$ and, for thiols, $\beta_{thiol} = 0.78\ n^{-1}$ (see Supporting Information). The lower value of β for dithiols is probably due to the fact that it is more probable to have several molecules participating in the junction for longer alkane-dithiols than for shorter ones, which raises the mean conductance value of the former.

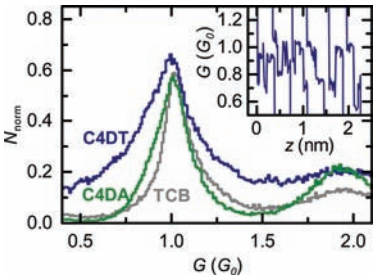

Figure 6. Conductance histogram at 1 G_0 in pure TCB and in the presence of C4DA and C4DT. The profile of the 1 G_0 peak is unchanged by the diamine, but becomes wider in the presence of the dithiol, due to the appearance of plateaus between 0.5 and 0.8 G_0 as shown in the G vs z traces for C4DT in the inset.

The histograms in Figure 4a,d include those traces with short plateaus for which the 1D histogram displays a flat background without molecular peaks. The L_{lp} values in this group are shorter for diamines than for dithiols, reflecting the staggered G decay observed for dithiols. The percentage of these traces without molecular-junction signature decreases linearly with the number of carbons from 55% for C3 to 5% for C8, regardless of anchor group. The values agree well with those previously reported for alkane diamines,[16] reflecting that long alkanes form stable junctions more easily than short ones. We observe the same success percentages for both diamines and dithiols, suggesting that the probability of forming junctions is the same for both binding groups. It is remarkable that for dithiols, the traces without plateaus show the same gold retraction hindrance as those with plateaus. This indicates that the effect does not depend on having molecules chemically bound to both electrodes. Cohesive forces, such a van der Waals or disuldife bonds, between molecules located on both electrodes may play a role. In addition, gold atoms that are covalently bonded to sulfur will not be as free to move on the surface anymore, and will also restrict the motion of neighboring atoms.

Our results show that, although the stronger bond of thiols to gold can seem in principle an advantage, alkane-dithiols produce greater changes in the electrode behavior and produce junctions with a larger number of participating molecules. On the other hand, alkane-diamines give more reproducible results and provide a more solid reference to compare with theoretical results.

1 G_0 Plateau Analysis. We can obtain a further insight into the effect of diamines and dithiols on the gold-atom rearrangement from analyzing the 1 G_0 plateaus. In the histogram of Figure 6, the profile of the 1 G_0 peak in the presence of C4DA is almost the same as in pure TCB. On the other hand, the tail of the peak extends down to 0.5 G_0 in the presence of C4DT. We observed the same result for all the studied dithiols, independently on the number of carbons in the chain (see 1D histograms on Figure S1). Looking at the individual traces for C4DT in Figure 6 (inset), we see that, in addition to the plateaus at 1 G_0, new plateaus appear between 0.5 and 0.8 G_0. Moreover, the presence of these plateaus results in longer stretching lengths between 1.2 and 0.5 G_0, L_{1G0} (Figure S9 in the Supporting Information), in agreement with the previous reports.[39,40]

We note that the presence of plateaus between 0.5 and 0.8 G_0 is uncorrelated with the appearance of molecular plateaus at lower conductance values (for example, the broadness of the 1 G_0 peak is the same in all the histograms of Sigure S7c), indicating

that these plateaus are not directly related with dithiols spanning the junction. They could be related to a sulfur at the end of an alkane-dithiol being inserted into the gold contact. Indeed, ab initio calculations suggest that an $-SCH_3$ bonded in the middle of a gold atomic contact can reduce the conductance down to 0.88 or 0.82 G_0.[41] A similar conductance change has been experimentally observed when other small molecules are embedded into the gold one-atom contact.[42]

CONCLUSIONS

In conclusion, our results show that the apparent stretching length L_S is determined not only by the length of the molecule, but also by the elastic and plastic deformations of the gold electrode contacts. These deformations can be considerably affected by the molecules attached to the electrodes, if their anchor groups bind strongly enough. This is an important effect to be taken into account when comparing different anchoring groups. Although a strong bond to the electrodes warrants stable molecular junctions, it can also mean severe changes to the electrode behavior. For the molecules studied in this work, we found that amines produce no apparent change in electrode behavior, which act as in the absence of molecules. However, thiols have a great impact on the deformations of the electrodes. The maximum stretching length for molecular junctions of alkane-dithiols can reach values almost double than the molecular length, suggesting that a large number of molecules participate in the junctions. These effects are also clearly observable in the region around 1 G_0, where more steps are visible in the presence of dithiols, while amines again produce no significant modifications. In all, alkane-diamines produce better defined junctions, which are more suitable as a reference model.

ASSOCIATED CONTENT

Supporting Information. Summary of length parameter definitions; one-dimensional conductance histograms; variation of the molecular conductance with the number of carbons; details on the calculations of the apparent stretching length, and the longest-plateau length; length distributions at 1 G_0. This material is available free of charge via the Internet at http://pubs.acs.org.

AUTHOR INFORMATION

Corresponding Author

teresa.gonzalez@imdea.org

Present Addresses

[§]Kavli Institute of Nanoscience, Delft University of Technology, 2600 GA Delft, The Netherlands.

[||]Departamento de Física de la Materia Condensada, Universidad Autónoma de Madrid, E-28049 Madrid, Spain.

ACKNOWLEDGMENT

This work was supported by the Spanish Ministerio de Ciencia e Innovación through the projects MAT2008-01735, RYC-2008-03328, and CSD2007-0010 (Consolider-ingenio, nanociencia molecular), the CAM through the project S2009/MAT-1726 (Nanobiomagnet), and the EU through the network FUNMOLS (Grant Number PITN-GA-2008-212942).

REFERENCES

(1) Agrait, N.; Yeyati, A.; van Ruitenbeek, J. *Phys. Rep.* **2003**, *377*, 81–279.

(2) Reed, M. A.; Zhou, C.; Muller, C. J.; Burgin, T. P.; Tour, J. M. *Science* **1997**, *278*, 252–254.

(3) Xu, B.; Tao, N. *Science* **2003**, *301*, 1221–1223.

(4) Cui, X.; Primak, A.; Zarate, X.; Tomfohr, J.; Sankey, O.; Moore, A.; Moore, T.; Gust, D.; Harris, G.; Lindsay, S. *Science* **2001**, *294*, 571–574.

(5) Haiss, W.; Nichols, R.; van Zalinge, H.; Higgins, S.; Bethell, D.; Schiffrin, D. *Phys. Chem. Chem. Phys.* **2004**, *6*, 4330–4337.

(6) Gonzalez, M. T.; Wu, S.; Huber, R.; van der Molen, S. J.; Schoenenberger, C.; Calame, M. *Nano Lett.* **2006**, *6*, 2238–2242.

(7) Li, X.; He, J.; Hihath, J.; Xu, B.; Lindsay, S. M.; Tao, N. *J. Am. Chem. Soc.* **2006**, *128*, 2135–2141.

(8) Fujihira, M.; Suzuki, M.; Fujii, S.; Nishikawa, A. *Phys. Chem. Chem. Phys.* **2006**, *8*, 3876–3884.

(9) Omori, Y.; Tobita, J.; Kato, Y.; Akiba, U.; Fujihira, M. *Jpn. J. Appl. Phys., Part 1* **2007**, *46*, 7829–7837.

(10) Martin, S.; Giustiniano, F.; Haiss, W.; Higgins, S. J.; Whitby, R. J.; Nichols, R. J. *J. Phys. Chem. C* **2009**, *113*, 18884–18890.

(11) Haiss, W.; Martin, S.; Leary, E.; van Zalinge, H.; Higgins, S. J.; Bouffier, L.; Nichols, R. J. *J. Phys. Chem. C* **2009**, *113*, 5823–5833.

(12) Li, C.; Pobelov, I.; Wandlowski, T.; Bagrets, A.; Arnold, A.; Evers, F. *J. Am. Chem. Soc.* **2008**, *130*, 318–326.

(13) Gonzalez, M. T.; Brunner, J.; Huber, R.; Wu, S.; Schoenenberger, C.; Calame, M. *New J. Phys.* **2008**, *10*, 065018.

(14) Venkataraman, L.; Klare, J. E.; Tam, I. W.; Nuckolls, C.; Hybertsen, M. S.; Steigerwald, M. L. *Nano Lett.* **2006**, *6*, 458–462.

(15) Park, Y. S.; Whalley, A. C.; Kamenetska, M.; Steigerwald, M. L.; Hybertsen, M. S.; Nuckolls, C.; Venkataraman, L. *J. Am. Chem. Soc.* **2007**, *129*, 15768–15769.

(16) Kamenetska, M.; koentopp, M.; Whalley, A. C.; Park, Y. S.; Steigerwald, M. L.; Nuckolls, C.; Hybertsen, M. S.; Venkataraman, L. *Phys. Rev. Lett.* **2009**, *102*, 126803.

(17) Huang, Z.; Chen, F.; Bennett, P. A.; Tao, N. *J. Am. Chem. Soc.* **2007**, *129*, 13225–13231.

(18) Tsutsui, M.; Shoji, K.; Taniguchi, M.; Kawai, T. *Nano Lett.* **2008**, *8*, 345–349.

(19) Tsutsui, M.; Taniguchi, M.; Kawai, T. *J. Am. Chem. Soc.* **2009**, *131*, 10552–10556.

(20) Xu, B. *Small* **2007**, *3*, 2061–2065.

(21) Quek, S. Y.; Kamenetska, M.; Steigerwald, M. L.; Choi, H. J.; Louie, S. G.; Hybertsen, M. S.; Neaton, J. B.; Venkataraman, L. *Nat. Nanotechnol.* **2009**, *4*, 230–234.

(22) Zhou, J.; Chen, G.; Xu, B. *J. Phys. Chem. C* **2010**, *114*, 8587–8592.

(23) Martin, C. A.; Ding, D.; Sorensen, J. K.; Bjornholm, T.; van Ruitenbeek, J. M.; van der Zant, H. S. J. *J. Am. Chem. Soc.* **2008**, *130*, 13198–13199.

(24) Chen, F.; Li, X.; Hihath, J.; Huang, Z.; Tao, N. *J. Am. Chem. Soc.* **2006**, *128*, 15874–15881.

(25) We estimate L_{mol} as the distance between the sulfur (nitrogen) centers, calculated for each fully stretched alkane with hyperchem, plus the maximum additional length that the Au−S bond could add, 2.5 Å (2.1 Å for the Au−N bond).

(26) Agrait, N.; Rubio, G.; Vieira, S. *Phys. Rev. Lett.* **1995**, *74*, 3995–3998.

(27) Rubio, G.; Agrait, N.; Vieira, S. *Phys. Rev. Lett.* **1996**, *76*, 2302–2305.

(28) Rubio-Bollinger, G.; Bahn, S.; Agrait, N.; Jacobsen, K.; Vieira, S. *Phys. Rev. Lett.* **2001**, *87*, 026101.

(29) Yanson, A.; Bollinger, G.; van den Brom, H.; Agrait, N.; van Ruitenbeek, J. *Nature* **1998**, *395*, 783–785.

(30) Untiedt, C.; Yanson, A.; Grande, R.; Rubio-Bollinger, G.; Agrait, N.; Vieira, S.; van Ruitenbeek, J. *Phys. Rev. B* **2002**, *66*, 085418.

(31) Olesen, L.; Brandbyge, M.; Sorensen, M.; Jacobsen, K.; Laegsgaard, E.; Stensgaard, I.; Besenbacher, F. *Phys. Rev. Lett.* **1996**, *76*, 1485–1488.
(32) Hihath, J.; Arroyo, C. R.; Rubio-Bollinger, G.; Tao, N.; Agrait, N. *Nano Lett.* **2008**, *8*, 1673–1678.
(33) Kim, Y.; Hellmuth, Th. J.; Marius Bürkle, M.; Pauly, F.; Scheer, E. *ACS Nano* **2011**, *5*, 4104.
(34) Xu, B.; Xiao, X.; Tao, N. *J. Am. Chem. Soc.* **2003**, *125*, 16164–16165.
(35) Ulman, A. *Chem. Rev.* **1996**, *96*, 1533–1554.
(36) Love, J.; Estroff, L.; Kriebel, J.; Nuzzo, R.; Whitesides, G. *Chem. Rev.* **2005**, *105*, 1103–1169.
(37) Porter, M.; Bright, T.; Allara, D.; CHidsey, C. *J. Am. Chem. Soc.* **1987**, *109*, 3559–3568.
(38) Huber, R.; Gonzalez, M. T.; Wu, S.; Langer, M.; Grunder, S.; Horhoiu, V.; Mayor, M.; Bryce, M. R.; Wang, C.; Jitchati, R.; Schoenenberger, C.; Calame, M. *J. Am. Chem. Soc.* **2008**, *130*, 1080–1084.
(39) Huisman, E. H.; Trouwborst, M. L.; Bakker, F. L.; de Boer, B.; van Wees, B. J.; van der Molen, S. J. *Nano Lett.* **2008**, *8*, 3381–3385.
(40) Sun, J.; Akiba, U.; Fujihira, M. *Ultramicroscopy* **2008**, *108*, 1034–1039.
(41) Hakkinen, H.; Barnett, R.; Landman, U. *J. Phys. Chem. B* **1999**, *103*, 8814–8816.
(42) Csonka, S.; Halbritter, A.; Mihaly, G. *Phys. Rev. B* **2006**, *73*, 075405.